Bulletin of the Seismological Society of America, Vol. 97, No. 5, pp. 1702–1717, October 2007, doi: 10.1785/0120050198

Probabilistic Seismic-Hazard Assessment for Portugal

by Susana P. Vilanova and Joao F. B. D. Fonseca

Abstract The probabilistic seismic hazard of Portugal is analyzed with a logic tree approach. A critical part of the work was the review of the seismic catalog and the moment magnitude (**M**) estimation for historical earthquakes. To produce a catalog with a uniform magnitude scale, the instrumental magnitudes were converted to **M** through empirical relations. Two seismic zonations were considered, each including two broad tectonic zones and a set of smaller seismicity zones. Catalog completeness and the *b*-value for the truncated exponential recurrence model were calculated for the broad sources defined by tectonic criteria. The smaller seismicity sources were used to calculate the *a*-value using the fixed *b*-value of the corresponding tectonic zone. This approach allows for a larger amount of data to estimate the most critical parameters by statistical methods, without compromising the spatial detail of hazard results. Three published attenuation relations were used in the logic tree, with weights that were based on tectonic considerations and on the comparison with macroseismic data converted to horizontal peak ground acceleration (PGA). The Ambraseys *et al.* (1996) attenuation model for PGA, used by most previous hazard studies of the region, seems to underestimate considerably the ground motion for mainland Portugal. A total of 96 hazard curves were calculated with SEISRISK III for each point of the map. The resulting mean hazard map for 10% exceedence probability in 50 years displays PGA values that range from 0.05*g* to 0.20*g*. These mean values are slightly higher than in previous PGA studies. The hazard patterns obtained display a maximum related to intraplate onshore seismicity, whereas previous studies using intensities highlighted the southwest offshore contribution. Further work on ground-motion attenuation in western Iberia is necessary to improve the seismic-hazard assessment.

Introduction

Mainland Portugal is located on the Eurasian plate in the vicinity of the southern boundary with the African plate, and its hazard is determined by large to very large offshore earthquakes and moderate to large onshore earthquakes (Moreira, 1989). The Azores-Gibraltar section of the boundary is well defined on its western part but becomes diffuse east of 13° W (Grimison and Chen, 1986; Buforn *et al.*, 1995), where the two plates converge obliquely in a northwest–southeast direction at a rate of 4 mm/yr (Argus *et al.*, 1989). This tectonic setting leads to significant onshore seismicity in western Portugal, the knowledge of which is mainly historical because no hazard-relevant earthquakes occurred after 1909. Because strong-motion data are nonexistent for significant earthquakes, most previous hazard studies of Portugal have relied on macroseismic information. Figure 1 shows the study region and surrounding area.

Structurally, the Iberian Peninsula exhibits the most continuous fragment of Hercynian basement in Europe (Ribeiro *et al.*, 1979) and acted as a nonvolcanic passive margin during the extensional phases that led to the opening of the Atlantic in the Mid Jurassic. The ocean-continent boundary (OCB) of the Western Iberia Margin is poorly known. Pinheiro *et al.* (1996) avoid the concept of OCB because the transition between oceanic and continental crust does not occur at a sharp boundary; in some places it consists of fragments of magmatically disrupted and thinned continental crust. The Tagus Abyssal Plain (TAP) is thought to be underlain in part by thinned continental crust and in part by oceanic crust (Pinheiro *et al.*, 1992), whereas the Gorringe Bank (GB), a seamount located southeast of TAP (Fig. 1) and traditionally associated with the 1755 Lisbon earthquake (e.g., Machado, 1966) is an uplifted fragment of oceanic crust (Feraud *et al.*, 1986). The old stable cratonic crust of Western Iberia has been characterized as possessing a low to very low macroseismic intensity attenuation, including the offshore region (Lopez Casado *et al.*, 2000).

Recognizing the difficulty in characterizing earthquakes not directly associated with plate boundaries and with large recurrence periods, Johnston and Kanter (1990) introduced the concept of "space for time substitution," meaning that

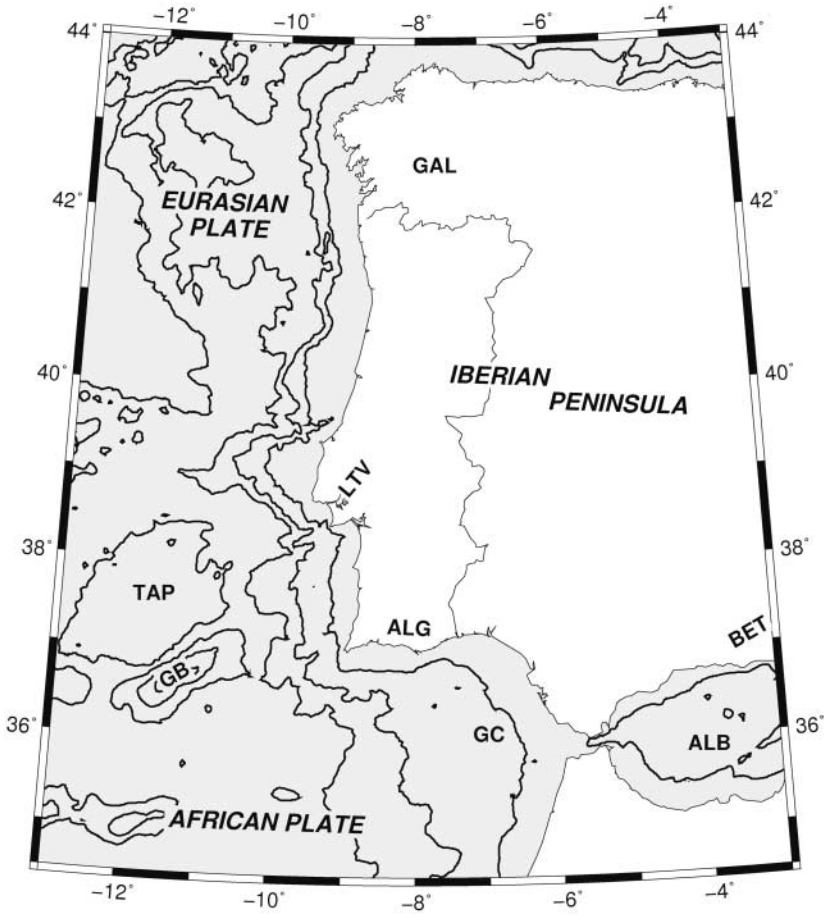

Figure 1. Western Iberia and surrounding area: ALB, Alboran Sea; ALG, Algarve Region; BET, Betic Chain; GAL, Galicia Region; GB, Gorringe Bank; GC, Gulf of Cadis; LTV, Lower Tagus Valley Region; TAP, Tagus Abyssal Plain.

the short (relative to the recurrence period) time record can be extended using data from worldwide regions with similar tectonic activity. Stable continental regions (SCRs) are defined as continental crust (including continental shelves, slopes, and attenuated continental crust) not deformed by large Mesozoic and Cenozoic orogenic processes, where tectonic activity is not directly related with plate boundary processes and which did not experience Neogene rifting, volcanism, or convergence (Johnston, 1989). The remaining continental regions are called active continental regions (ACRs). SCRs exhibit low heat flow, low deformation rates, and low anelastic attenuation of seismic waves compared with ACRs. The latter property has important implications in the retrieval of information from historical data because the severity and damage extent of historical earthquakes is obviously dependent on crustal attenuation characteristics. Also, the use of ground-motion models derived empirically in ACRs to estimate SCR ground motions is not adequate. Johnston (1996a,b,c) evaluated systematically worldwide SCR earthquakes providing empirical relations to estimate seismic moment M_0 from either macroseismic information or instrumental magnitudes.

In the present study we invoke the "space for time substitution" concept to estimate the moment magnitude of historical and instrumental earthquakes and to judge the appropriateness of attenuation models proposed for other regions. We use a new hazard-purpose catalog and devote particular attention to the analysis of its completeness and the calculation of exponential recurrence parameters. The hazard results are presented and analyzed with a logic tree approach.

Historical and Instrumental Seismicity

In regions of moderate tectonic activity, where as a rule the seismogenic processes are relatively unknown and the ground-motion data sparse, seismicity is the major input for seismic-hazard analysis, often complemented with paleoseismological data to cover the longer return periods and estimate maximum expected magnitude. In Portugal, the latter type of data is very sparse, with only a few exceptions. Most published studies focus on neotectonic deformation (Cabral, 1989, 1995) and derive average slip rates for the past 3.5 million years, a period that is too long for seismic-hazard assessment (McCalpin, 1996).

Based on trenching near Lisbon, Fonseca *et al.* (2000) reported Holocene deformation on the Lower Tagus Valley fault system, which has been associated with the historical seismicity of the region (Justo and Salwa, 1998). However, that interpretation has been controversial (Cabral and Marques, 2001) and further fieldwork (currently underway) is

required before the results can be used to characterize earthquake recurrence. Only for the Vilarica strike-slip fault, in the low-hazard northeast of the country, conclusive paleoseismological results were achieved in the scope of a dam site investigation, yielding a slip rate in the range 0.2–0.7 mm/yr and a maximum magnitude of **M** 7.25 with a return period of about 9000 years (Rockwell *et al.*, 2005). Although we stress the importance of active tectonics and paleoseismology for hazard assessment in a region of moderate seismic activity such as Portugal (Vilanova and Fonseca, 2004), we are forced by the lack of available data to conduct the present study on the basis of historical and instrumental data only. We analyzed the available seismicity catalogs for the region to retrieve the most relevant information for a hazard-purpose catalog.

Available Seismicity Catalogs

The most recent seismicity catalog for Portugal (Sousa *et al.*, 1992) is a compilation of previous catalogs, complemented with instrumental data from the national Portuguese seismic network. The events are assigned the magnitudes available in the original catalogs: body wave (m_b), surface wave (M_S), local magnitude (M_L), and an unspecified magnitude named M_p in that publication. The use of the M_p magnitude is related to the fact that one of the sources used in the compilation, the catalog of Martins and Mendes-Victor (1990), presents no information on the magnitude type. Numerous historical earthquakes (since 63 B.C.) are characterized with M_p magnitudes. The original source of most M_L is the Instituto Geografico Nacional (Spain) catalog (IGN, 1992). The magnitudes m_b and M_S are not well represented in the region and are available only for larger-magnitude events.

The IGN (1992) catalog is an updated version of the catalog of Mezcua and Martinez Solares (1983) for the Ibero-Maghreb region. The historical period extends back to the beginning of the twentieth century and for these earthquakes, Mezcua and Martinez Solares (1983) estimated epicentral locations and, when enough information was available, macroseismic intensities Medveder–Sponheuer–Karnik (MSK) (in general, no intensities were estimated for events prior to the fifteenth century).

For the instrumental period after 1962, Mezcua and Martinez Solares (1983) calculated earthquakes magnitudes using the maximum amplitude of the *Lg* wave calibrated with the body-wave magnitudes m_b given by the National Earthquake Information Service of U.S. Geological Survey (USGS). The relations used were based on short-period records (vertical component) of 30 earthquakes geographically distributed throughout the Iberian Peninsula and recorded at different stations during the period 1964–1975. For the period 1924–1962, Mezcua and Martinez Solares (1983) used the duration magnitude, calibrated with the post-1962 m_{bLg} magnitudes.

The catalog of Oliveira (1986) is a detailed review of the historical seismicity of Portugal. The estimated parameters (intensity, epicentral location, magnitude, etc.) are characterized by an index according to the quality of original historic reports. A large subset of the historical earthquakes on the catalog of Sousa *et al.* (1992) characterized by unspecified magnitude correspond to M_L estimated by Oliveira (1986) using the classical epicentral intensity-magnitude relation of Gutenberg and Richter.

The Working Catalog

This section describes the options used in the construction of the working catalog, namely for source catalog, magnitude homogenization, and epicentral location.

The main option was to use a moment magnitude (**M**)-based catalog. Other magnitude scales were converted to seismic moment through recent empirical relationships, and then to **M**, using the Hanks and Kanamori (1979) relationship.

The IGN catalog (IGN, 1992), complemented with data from the same institution for the period 1990–2000, was used as the basis for the instrumental catalog. The magnitudes m_{bLg} routinely calculated by IGN for this period use the formula derived by Mezcua and Martinez Solares (1983) (Centre Sismologique Euro-Mediterraneen/European-Mediterranean Seismological Centre [CSEM/EMSC], 1999). Whenever available (usually for larger-magnitude events) we preferred teleseismic magnitudes and **M** provided by the International Seismological Centre (ISC, 2001).

Johnston (1996a) presents empirical regressions to convert both teleseismic (M_S and m_b) and regional magnitudes (m_{bLg} and M_L) to M_0 (dyn cm) for stable continental crust earthquakes. The relationships for teleseismic magnitudes are

$$\log M_0 = 24.66 - 1.083\, M_S + 0.192\, M_S^2 \quad \text{for } M_S \geq 3.6 \qquad (1)$$

$$\log M_0 = 18.28 + 0.679 m_b + 0.077 m_b^2 . \qquad (2)$$

Although derived from a specific SCR database, these relationships are in agreement with global regressions and expected theoretical slopes. The advantage in using these relationships is that they include a thorough error analysis that can be used to rank events in terms of magnitude quality and reliability.

Figure 2a and b plot **M** versus m_b and M_S, respectively, for earthquakes in the Iberian region for which **M** is available from international agencies (ISC, 2001). The data used is presented in Table 1. Independently of tectonic region, m_b and $M_S \geq 4.0$ show good agreement with SCR relationships represented by equations (1) and (2). The relation proposed by Johnston (1996a) for m_{bLg} is not suitable for IGN m_{bLg} data. Figure 2c displays the IGN m_{bLg} post-1983 data versus m_b data indicating that, although there is some dispersion, no relevant bias exists between both scales. Therefore these data were converted to M_0 through equation (2).

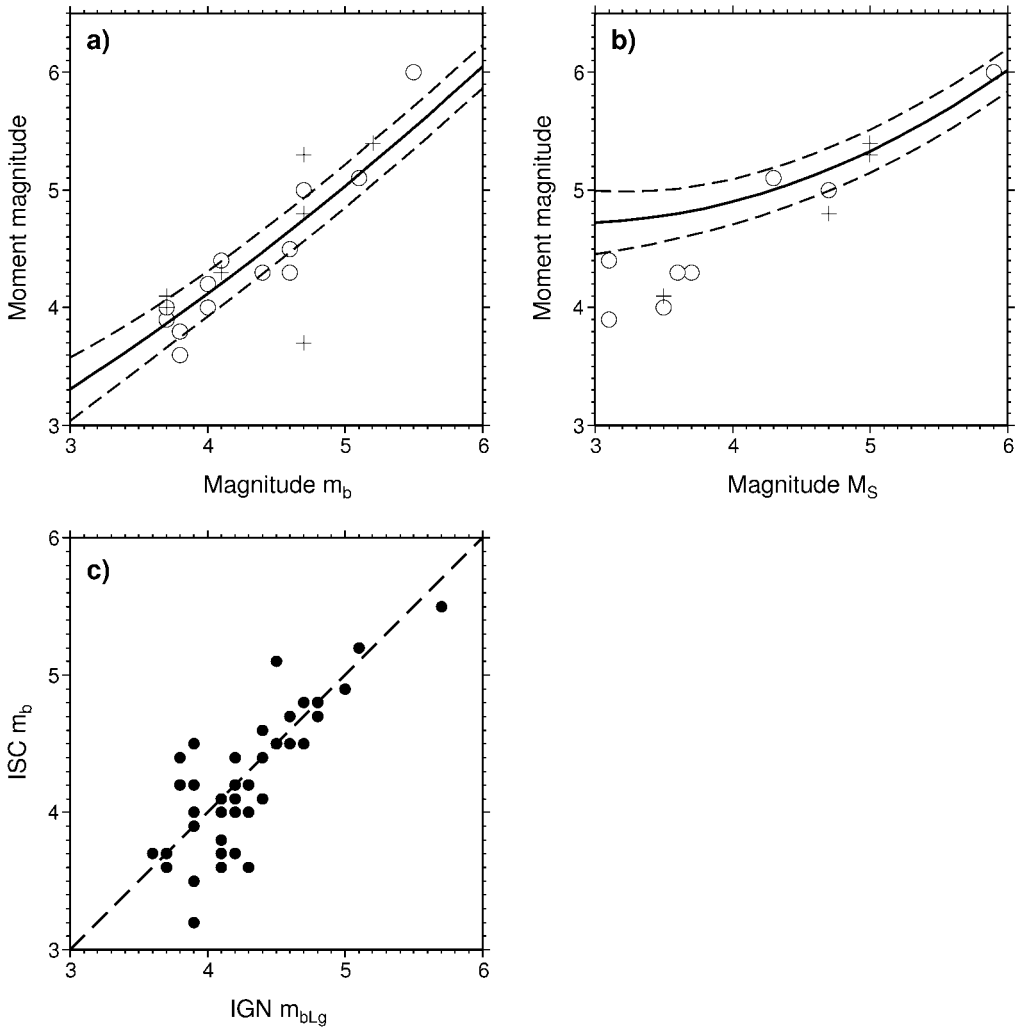

Figure 2. Earthquakes in the Iberian region with teleseismic magnitudes and moment magnitude published by ISC (2001): (a) M_S versus **M** and equation (1) with associated prediction error (1σ); ACR data are represented with open circles and SCR data with crosses. (b) m_b versus **M** and equation (2) with associated prediction error (1σ); ACR data are represented with open circles and SCR data with crosses. (c) m_{bLg} from IGN versus m_b for post-1983 events; the dashed line represents 1:1 relationship.

According to the guidelines of Johnston (1996a), when **M** was not available, we used preferentially M_S magnitudes to retrieve M_0 for $M_S \geq 5.5$, teleseismic magnitudes M_S and m_b (a weighted mean if both available; no $M_S < 4.0$ were used), and finally, regional IGN $m_{bLg} \geq 3.5$. The associated errors in **M** derived from instrumental magnitudes are in the range 0.10 to 0.30. The largest event of the instrumental period, the 28 February 1969 Gorringe Bank earthquake (M_S 7.8; Fukao, 1973), was assumed to be a **M** 7.8 in size.

For the preinstrumental catalog the choice was to retrieve macroseismic data to estimate the **M** through empirical relations. The catalog of Oliveira (1986) was the main reference for these earthquakes. The events with quality factors for epicentral location and macroseismic intensity "good" or "medium" and modified Mercalli intensity (MMI) $\geq$ VI were selected (about 15% of the total). The selected dataset was complemented by the events on IGN's (1992) catalog for which an isoseismal map was available. In addition, the isoseismals of Justo and Salwa (1998) were used to estimate the moment magnitude of the 26 January 1531 earthquake. Although Justo and Gentil (1990) provide isoseismals for the 24 August 1356 earthquake, these were not used because they are poorly constrained by the coeval data.

The M_0 estimate was performed with the Johnston (1996b) empirical model using isoseismal areas, yielding for the analyzed earthquakes errors in the range 0.30–0.40 units of **M**. When an isoseismal map was not available, the M_0 was estimated through the maximum intensity model of Johnston (1996b). In this case the errors increase to 0.50–0.52 units of **M** for the studied earthquakes. For the distant offshore historical earthquakes, the data do not support more accurate magnitude estimates and therefore the values pro-

posed by Oliveira (1986) or by Moreira (1979) were used. Further details can be found in Vilanova (2004).

There are three exceptions to this procedure: the 5 April 1504 Carmona earthquake, the 1 November 1755 "Lisbon Earthquake," and the 23 April 1909 Benavente earthquake. The 5 April 1504 earthquake produced a surface rupture with 1.8 m of maximum displacement (Udias *et al.*, 1976) which yields **M** 6.9 ± 0.4 by the empirical relations of Wells and Coppersmith (1994).

The location of the 1 November 1755 has been widely discussed and proposed sources are located over a large area from offshore Lisbon to the Gulf of Cadiz (see Fonseca, 2005, for a discussion). Johnston (1996c) proposes **M** 8.7 ± 0.4 based on isoseismal areas calibrated with the macroseismic field of 28 February 1969. Intensities MM larger than VIII were not used, which is actually a desirable procedure because the distribution of high intensities is controversial and displays an intriguing shape. A lobe of high intensities near Lisbon has been tentatively explained with a moderate-magnitude event close to Lisbon, triggered by the main offshore earthquake (Vilanova *et al.*, 2003). Martinez Solares and Lopez Arroyo (2004) use the methodology proposed by Johnston (1996c) together with a more accurate intensity map and a different approach to extrapolate offshore isoseismal areas, leading to the value **M** 8.5 ± 0.3. We adopt the value of Martinez Solares and Lopez Arroyo (2004).

Table 1
Data from ISC (2001) Used in Figure 2a and b

Date	Time	**M**	Agency	M_S	Agency	m_b	Agency
1986/10/20	14:48:19.8	5.0	IAG	4.7	ISC	4.7	ISC
1988/07/25	20:03:08.8	4.5	IAG	–	–	4.6	ISC
1994/05/26	08:26:53.1	6.0	HRV	5.9	ISC	5.5	ISC
1997/05/21	23:50:42.7	5.4	HRV	5.0	ISC	5.2	ISC
1997/05/21	23:49:42.3	5.3	HRV	5.0	ISC	4.7	ISC
1997/05/22	00:17:17.9	4.8	MED	4.7	ISC	4.7	ISC
1997/05/22	05:06:49.3	4.3	IAG	–	–	4.1	ISC
1997/08/20	02:44:02.2	4.0	IAG	2.9	ISC	3.7	ISC
1998/04/13	05:55:42.6	3.6	IAG	–	–	3.8	MDD
1998/07/17	08:29:02.3	4.0	IAG	–	–	3.7	ISC
1999/07/18	17:26:46.7	3.9	IAG	3.1	EIDC	3.7	ISC
1999/08/04	09:02:54.6	4.3	IAG	3.7	ISC	4.4	ISC
1999/11/10	13:10:12.1	4.4	MED	3.1	EIDC	4.1	ISC
2000/07/05	09:26:49.9	4.0	ZUR	3.5	ISC	4.0	ISC
2001/05/20	01:39:06.9	3.7	IAG	–	–	4.7	ISC
2002/03/28	04:09:27.6	3.8	IAG	–	–	3.8	ISC
2002/06/27	13:29:51.8	3.8	IAG	–	–	–	–
2002/08/24	10:08:08.9	4.2	IAG	2.5	LDG	4.0	ISC
2002/09/15	20:54:17.3	4.1	IAG	2.9	LDG	–	–
2002/12/10	13:51:32.4	5.1	HRV	4.3	–	5.1	ISC
2003/01/12	15:56:32.1	3.8	IAG	–	–	–	–
2003/01/23	10:13:14.4	4.1	ZUR	3.5	ISC	3.7	ISC
2003/01/24	20:34:58.5	4.3	ZUR	3.6	–	4.6	ISC
2003/07/18	21:23:14.5	4.0	IAG	–	–	3.7	ISC
2003/07/25	03:37:54.8	3.5	IAG	–	–	–	–
2005/02/20	13:26:01.0	3.7	IAG	–	–	–	–

The reporting agency according to ISC (2001) is displayed for each assigned magnitude.

For the 23 April 1909 event we used **M** 6.27 ± 0.18, obtained through equation (1) considering M_S 6.30 ± 0.25, as calculated by Dineva *et al.* (2002) using surface waves recorded at 19 stations. The same authors obtained also **M** 6.18 ± 0.18 from long-period spectra of three records, whereas the isoseismal areas yield a value of **M** 6.37 ± 0.23. The fact that the latter value is consistent with those derived from instrumental records is a possible indication of the applicability of isoseismal relationships of Johnston (1996a) to the studied area.

Table 2 lists earthquakes with $M \geq 5.5$ used in the study. To account for the magnitude uncertainty we used two versions of the catalog, CA and CB, the former including all data and the latter including events with magnitude error not exceeding 0.4 (in practice this excludes magnitudes derived from maximum intensity). The two options correspond to separate branches of the logic tree.

Source Zone Characterization

We used two sets of source zones. In both cases the region was divided in two broad zones, corresponding to the ACR and the SCR, according to the criteria of Johnston

Table 2
Working Catalog: Seismicity with **M** ≥5.5

Date	Time	Longitude	Latitude	**M**	σ	Note*
1344/–/–	—	−9.20	38.70	6.70	0.50	J96(Imax)
1353/01/–	—	−8.10	37.30	5.50	0.50	J96(Imax)
1356/08/24	—	−10.70	36.00	7.50	1.00	LNEC86
1504/04/05	09:–:–	−5.60	37.40	6.90	0.40	WC94-MDall
1531/01/26	—	−9.00	38.95	6.90	0.30	J96(isos)
1587/11/–	—	−8.00	37.10	5.50	0.50	J96(Imax)
1719/03/06	05:–:–	−10.70	36.00	7.00	1.00	LNEC86
1722/12/27	17:30:–	−7.58	37.17	6.90	0.30	J96(isos)
1755/11/01	09:–:–	−10.50	36.00	8.50	0.30	MMS04
1761/03/31	12:05:–	−10.50	36.00	7.50	1.00	LNEC86
1777/04/12	05:15:–	−10.00	36.00	7.00	1.00	LNEC86
1856/01/12	11:20:–	−8.00	37.10	5.50	0.50	J96(Imax)
1858/03/19	13:30:–	−7.00	41.20	5.80	0.30	J96(isos)
1858/11/11	07:15:–	−9.00	38.20	7.100	0.30	J96(isos)
1903/08/09	22:10:10.0	−9.00	38.30	6.50	0.30	J96(isos)
1909/04/23	17:39:36.8	−8.82	38.95	6.27	0.18	J96(MS)
1915/07/11	11:29:16.0	−11.80	35.50	6.27	0.27	J96(MS)
1930/07/05	23:11:44.0	−4.63	37.62	5.79	0.18	J96(MS)
1934/11/12	08:31:15.0	−7.83	37.75	5.79	0.18	J96(MS)
1941/12/27	18:17:38.0	−10.00	35.80	6.70	0.19	J96(MS)
1964/03/15	22:30:26.9	−7.75	36.13	6.27	0.27	J96(mb)
1967/05/17	20:14:07.8	−4.31	37.79	5.74	0.26	J96(mb)
1969/02/28	02:40:32.7	−10.81	35.99	7.80	0.10	F73
1994/05/26	08:26:53.1	−4.00	35.27	6.00	0.10	ISC

*The methodology used to estimate **M** was: LNEC86, after Oliveira (1986); J96(Imax), regression using maximum intensity of Johnston (1996b); J96(isos), regressions using isoseismal areas of Johnston (1996b); J96(MS), regression using M_S of Johnston (1996a); J96(mb), regression using m_b of Johnston (1996a); WC94-MDall, regression on average displacement (all fault types) of Wells and Coppersmith (1994); MMS04, after Mezcua and Martinez Solares (2004); F73, after Fukao (1973); ISC, reported in ISC (2001).

(1989) (Fig. 3). For practical reasons a small portion of oceanic crust, around the Gorringe Bank, was included in the western part of the ACR. These broad zones were subdivided in smaller sources in two different ways. Zonation SA comprises 11 source zones based on seismicity criteria: in regions where local moderate to large historical earthquakes occurred the source area boundaries follow roughly the isoseismal VIII (MMI), because the area enclosed by this relatively high damage distribution is likely to include the geological source, and in every other region they comprise diffuse seismicity areas. Zonation SB comprises eight source zones adapted from the proposal of Pelaez and Lopez Casado (2002) (we divided their broad zone IOb1, including Central and Southern Portugal, into eastern and western regions). Figure 3 shows the two zonations, together with the historical and instrumental seismicity of the region.

The recurrence rates were calculated with two alternative methods (designated by RA and RB), forming two branches of the final hazard logic tree. Since the amount of data within some source zones does not support a robust statistical analysis, in both approaches the completeness period and *b*-value estimates were performed globally for each broad tectonic region. The ACR includes a large offshore region with a higher seismicity rate than the onshore SCR. Therefore a large part of the instrumental data comes from ACR, whereas most of the historical data come from SCR, making it convenient to calculate completeness and *b*-values separately for each zone. The *b*-value calculations were performed with the maximum likelihood method for variable observation periods of Weichert (1980).

Method RA is based on the completeness analysis proposed by Stepp (1972) which assumes that earthquake occurrence is a poissonian process and consequently the variance of the λ parameter estimator is inversely proportional to the length of the observation period. The analysis was performed for each broad tectonic region and at intervals of 0.1 units of magnitude, and according to the result the magnitude values were grouped in different completeness classes. Represented by t_i the completeness interval for magnitude m_i and by t_{i+1} the interval for magnitude $m_i + 0.1$, if $t_i \approx t_{i+1}$ both values of magnitude were included in the t_i interval, otherwise a new completeness interval was initiated with period t_{i+1}. The recurrence rates for each magnitude and the corresponding completeness period were then used to calculate the *b*-value. Finally, the recurrence rates for each seismicity zone were calculated using the fixed *b*-value for the corresponding tectonic zone.

When the entire catalog (CA) was analyzed with method RA, SCR data showed a sharp positive offset on the Stepp (1972) plot, indicating a strong nonpoissonian behav-

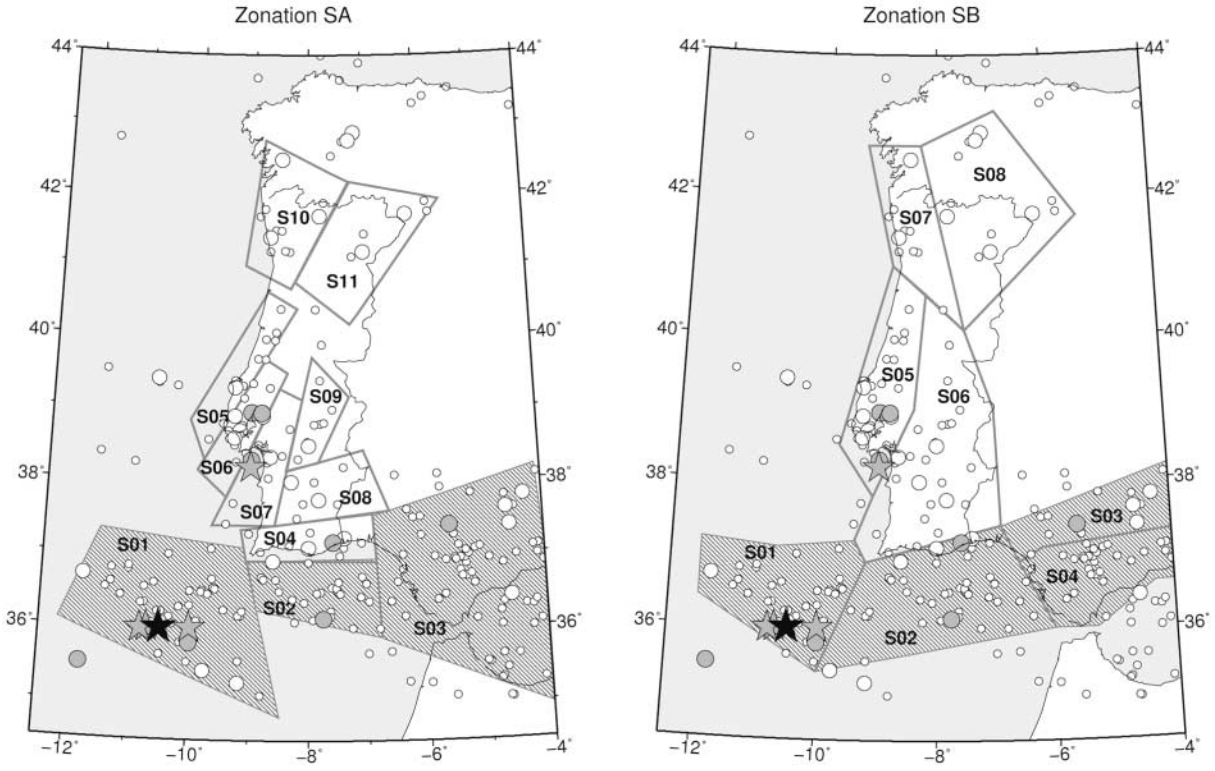

Figure 3. Zonations used and the working catalog. The stripped pattern highlights ACR source zones. The seismicity is represented as follows: $4 \leq \mathbf{M} < 5$, small open circles; $5 \leq \mathbf{M} < 6$, open circles; $6 \leq \mathbf{M} < 7$, gray circles; $7 \leq \mathbf{M} < 8$, gray stars; $\mathbf{M} > 8$ (1755 "Lisbon" earthquake), filled star.

ior. This anomaly results clearly from the inclusion of events with magnitude calculated from the maximum intensity relationship (associated error exceeding 0.4) and therefore a less accurate estimate of its value. We choose a completeness period that excluded events presenting this behavior.

Method RB uses the technique proposed by Albarello *et al.* (2001) for completeness analysis. The idea underlying the method is that a complete and representative catalog exhibits similar statistical properties in its first and second halves. A completeness probability-density function is calculated at discretized values T_i of completeness period dividing the period $\Delta T_i = T_{\text{present}} - T_i$ in $2N$ intervals and comparing the first and second halves. In this way Albarello *et al.* (2001) estimate the probability that the analyzed period is complete.

The magnitude range was divided in intervals of 0.3 units starting at **M** 4.0 and the completeness probability density function was calculated for each tectonic region and for each magnitude interval. A trial for magnitude intervals of 0.5 units gave very similar results. The timestep $\delta t = \Delta T_i/N$ for the analysis has a larger influence: for the catalog used and for magnitudes below **M** 7.0 the parameter δt between 1 and 10 gives reasonable results, whereas for greater magnitudes the timestep between 50 and 100 is a better choice. In any case, the results for larger magnitudes are not very reliable, as expected given the limited number of events. We used $\delta t = 10$ for magnitudes bellow **M** 7.0 and $\delta t = 100$ above that value. The recurrence rates for the *b*-value calculation were obtained by the weighted mean of the recurrence rates (running through the completeness period). The recurrence rates for each seismicity zone were calculated through the rates of magnitude above the minimum magnitude m_0 weighted by the completeness probability-density function of the corresponding broad tectonic region.

To minimize the impact of the fixed *b*-values when applied to each seismicity zone, in both methods (RA and RB) we calculated the *a*-values using two different minimum magnitudes **M** 4.0 and **M** 4.6, following the methodology suggested by Frankel (1995).

The results for the two zonations are summarized in Tables 3 and 4. Concerning the *b*-value, both methods gave similar results. The technique of Albarello *et al.* (2001), once calibrated, reduces considerably the subjective decisions made by the analyst. It also shows little sensitivity to the inclusion of lower-quality data (branch B-C2). The *b*-value obtained for the ACR is slightly higher than that obtained for the SCR, independently of the completeness method used.

The frequency-magnitude relations obtained are within the range of published results for different tectonic settings. In Triep and Sykes (1997), *b*-values for ACR are usually lower than *b*-values for SCR. However, *b*-values for European ACR ($b = 1.08 \pm 0.37$) are higher than ACR values in general and closer to the values for overall SCR (no values for European SCR are presented). There is good agreement between the values calculated in the present study and those given by Triep and Sykes (1997).

Table 3
Parameters *a* and *b* for Zonation SA Using Analysis Methods RA and RB (with Variants CA and CB)

	CA			CB			
Source Zone	a_1	a_2	b	a_1	a_2	b	$M_{\max}$
			RA				
S01	4.14	4.12		3.77	3.72		8.5
S02	3.77	3.96	1.03	3.41	3.57	0.94	6.3
S03	4.18	3.99		3.82	3.60		6.9
S04	3.02	2.70		2.89	2.75		6.9
S05	2.88	2.67		2.71	2.48		5.0
S06	2.88	3.03		2.74	2.92		6.9
S07	2.92	2.78	0.94	2.75	2.58	0.89	7.1
S08	2.85	2.64		2.68	2.44		5.3
S09	2.37	2.53		2.19	2.33		5.8
S10	2.70	3.03		2.58	2.92		5.2
S11	2.76	2.76		2.59	2.56		5.8
			RB				
S01	4.55	4.63		4.46	4.53		8.5
S02	4.16	4.46	1.13	4.07	4.35	1.10	6.3
S03	4.56	4.40		4.47	4.31		6.9
S04	3.40	3.29		3.33	3.34		6.9
S05	3.28	3.33		3.17	3.21		5.0
S06	3.31	3.42		3.24	3.40		6.9
S07	3.25	3.40	1.02	3.14	3.25	0.99	7.1
S08	3.33	3.16		3.24	3.17		5.3
S09	2.70	2.87		2.81	3.19		5.8
S10	3.17	3.47		3.11	3.44		5.2
S11	3.15	3.26		3.04	3.10		5.8

The *a*-values calculated using **M** ≥4.0 are labeled a_1, and using **M** ≥4.6 a_2. See text for explanation.

Ground-Motion Characterization

As in most moderate-seismicity regions, the ground-motion database of Mainland Portugal is composed of small-magnitude events (**M** 2.7–4.0) at short to medium distances (10–200 km), moderate-magnitude events (**M** 5.0–5.3) at medium to large distances (80–450 km), and one large event (**M** 7.8) at a large distance (332 km). The moderate- to large-magnitude events that affected the region occurred prior to the instrumental period and its effects are characterized in terms of intensity. In the absence of ground-motion models for the studied region, to perform the analysis in terms of peak ground motion acceleration it is necessary to rely on studies developed for regions with similar crustal characteristics, following the "space for time" approach of Johnston and Kanter (1990).

Attenuation Models

We analyzed several ground-motion models and included three models in the logic tree: Ambraseys *et al.* (1996), Toro *et al.* (1997), and Atkinson and Boore (1997). These models where chosen because the data used to derive them included large magnitudes and large distances (the historical seismicity of the region under study reaches **M** 8.5

Table 4
Parameters *a* and *b* for Zonation SB Using Analysis Methods RA and RB (with Variants CA and CB)

	CA			CB			
Source Zone	a_1	a_2	b	a_1	a_2	b	M_{max}
			RA				
S01	3.78	3.72		3.77	3.70		8.5
S02	3.42	3.57	0.94	3.41	3.54	0.94	6.9
S03	3.82	3.60		3.82	3.58		6.9
S04	3.00	2.86		2.97	2.68		6.0
S05	2.79	2.57		2.79	2.57		7.1
S06	2.82	3.01	0.91	2.78	2.93	0.91	5.8
S07	2.83	2.68		2.83	2.68		5.2
S08	2.76	2.53		2.76	2.53		5.8
			RB				
S01	4.35	4.34		4.45	4.45		8.5
S02	4.25	4.47	1.09	4.35	4.58	1.12	6.9
S03	3.78	3.79		3.88	3.92		6.9
S04	4.17	3.90		4.26	3.96		6.0
S05	3.53	3.67		3.58	3.70		7.1
S06	3.63	3.63	1.00	3.69	3.65	1.02	5.8
S07	3.12	3.45		3.14	3.43		5.2
S08	3.51	3.61		3.59	3.71		5.8

The *a*-values calculated using $\mathbf{M} \geq 4.0$ are labeled a_1 and using $\mathbf{M} \geq 4.6$ a_2. See text for explanation.

offshore and **M** 7.1 in the stable continental crust). Also, the target areas are not too specific: Europe and the Middle East in one case, Central and Eastern North America (CENA) in the other two.

The ground-motion model of Ambraseys *et al.* (1996), the one most used throughout Europe, was developed using data from the most active part of Europe and the Middle East (e.g., Italy, Greece, Turkey). This is a tectonically complex region dominated by the collision between Eurasian, African, and Arabian Plates (e.g., McKenzie, 1970). The central Italy region is under extension, and further east, the deformation is accommodated by major strike-slip fault systems, leading to the extrusion of the Anatolian microplate and its subduction under the Hellenic trench. Because this tectonic framework shows striking differences with the region under analysis, the respective ground-motion model is considered, *a priori*, less appropriate than the SCR models discussed next. This model uses M_S instead of **M** and therefore needs adequate conversion.

We used two SCR ground-motion models developed for CENA using simulated data based on the stochastic source model, namely Toro *et al.* (1997) and Atkinson and Boore (1997). We chose CENA models because North Atlantic margins share a common geologic evolution: the cratonic basement affected by a dense network of faults (the Megashear Zone of Arthaud and Matte, 1977) underwent Early Mesozoic rifting and extension during the opening of the North Atlantic Ocean. Neither region experienced major deformation associated with Cenozoic orogenic processes and both are currently under compression. Atkinson and Boore (1997) scaled their model using regional small to moderate events, along with teleseismic spectra from worldwide intraplate events.

For the **M** 6.3 earthquake of 23 April 1909 at Benavente, near Lisbon, the magnitude estimated with instrumental data (Dineva *et al.*, 2002) is in good agreement with that obtained using the isoseismal area regressions of Johnston (1996b), a further indication that CENA and West Iberia attenuation laws are similar. Lopez Casado *et al.* (2000) analyzed mean isoseismal radii of historical earthquakes felt in the Iberian Peninsula and concluded that the westernmost region, including Portugal, the Cadiz Gulf, and Galicia, has very low attenuation. In contrast, other active tectonic regions like the Betic Chain or the Pyrenees (not included in the present study) display high to very high attenuation.

Lopez Casado *et al.* (2000) relate this difference with the contrast between the cratonized crust in the west and crust densely fractured by the Alpine Orogeny in the east. In view of these findings we used the same attenuation models for both ACR and SCR zones, assuming that in both regions the crust transmits seismic energy efficiently, and therefore the attenuation is comparable to that of SCR in general.

The attenuation models and application domains are described in Table 5.

Regional Ground-Motion Data

The strong-motion database does not provide constraints on ground-motion models, because the stronger earthquakes recorded in the accelerometer network are in the range **M** 4.7–5.3. The only exception, the 28 February 1969 M_S 7.8 earthquake, was recorded at a bridge cable anchorage, in Lisbon, 332 km away from the epicenter. We complemented the Portuguese ground-motion database with Spanish free-field data of earthquakes within the region of interest (Ambraseys *et al.*, 2002). Table 6 presents recorded ground-motion data for shallow earthquakes within the application domain of at least one of the adopted models. No ground-motion record is actually within the application domain of all models.

Figure 4 presents the residuals of the natural logarithm of the ground-motion data with respect to the values predicted by the selected models, for **M** 4.7–7.8 earthquakes recorded up to 500 km. A large dispersion is observed for all analyzed models. The models of Atkinson and Boore (1996) and Ambraseys *et al.* (1996) show a good fit to the data at large distances (offshore earthquakes) whereas the model of Toro *et al.* (1997) underpredicts most of the data at long distances. Data in the range 10–30 km show good agreement with the model of Ambraseys *et al.* (1996).

Regional data on the effects of earthquakes with engineering interest are mostly intensity data, and it is therefore tempting to convert these data to PGA for comparison with the ground-motion models. However, difficulties in this con-

Table 5
Application Domains and Relationships for the Attenuation Models Considered

Model	**M**	Distance (km)	Parameter
a	[4.0, 7.2]	$10 \leq r_h \leq 500$	PGA maximum horizontal component
b	[5.0, 8.0]	$1 \leq d \leq 500$	PGA maximum horizontal component
c	[4.9, 7.5]*	$d \leq 200$	PGA random horizontal component

Model	Function
a	$\ln(\text{PGA}) = 1.841 + 0.686(\mathbf{M} - 6) - 0.123(\mathbf{M} - 6)^2 - \ln(r_h) - 0.00311 r_h$
b	$\ln(\text{PGA}) = 2.20 + 0.81(\mathbf{M} - 6) - 1.27 \ln(r_b) + 0.11 \max(r_b/100, 0) - 0.0021 r_b$, $r_b = \sqrt{(d^2 + 9.3^2)}$
c	$\log_{10}(\text{PGA}) = -1.48 + 0.266 M_S - 0.922 \log_{10}(r_c)$, $r_c = \sqrt{(d^2 + 3.5^2)}$

Models: (a) Atkinson and Boore (1997); (b) Toro *et al.* (1997) for Midcontinent; and (c) Ambraseys *et al.* (1996). Variables r_h and d correspond to hypocentral distance and closer distance to the fault area projection on surface. PGA is in units of g.

*Converted from M_S through Johnston (1996a).

Table 6
Regional Ground-Motion Data with **M** >4.7 Recorded within 500 km from Epicenter in Free-Field (ff) or in Ground Level of up to Two-Story Buildings (1s stands for 1-story and 2s for 2-story buildings)

Date	Time	**M**	M_S	Build.	Geol.	Ep. Dist. (km)	PGA (cm sec^{-2})	Ref.
1969-02-28	02:40:31	7.8	7.8	ca	alluv.	332	25.8	a
1989-12-20	04:15:00	5.0*	4.7	ff	stiff s.	16	57.2	a
1997-05-23	18:14:39	4.7*	3.8*	ff	stiff s.	5	146.5	a
				ff	stiff s.	28	15.4	a
2002-12-10	13:51:32	5.1	4.3	1s	alluv.	79	2.44	b
2003-07-29	05:31:27	5.3	4.8	2s	rock	236	7.9	b
				ff	rock	256	2.8	b
				1s	stiff s.	336	2.5	b
				2s	soft s.	443	4.0	b
2004-12-13	14:16:08	5.0	4.3	1s	alluv.	313	5.8	b
				1s	stiff s.	267	4.0	b
				1s	rock	344	2.5	b
				1s	rock	164	10.3	b
				ff	stiff s.	277	3.8	c
				ff	stiff s.	294	2.0	c
				ff	—	318	2.5	c

The 1969-02-28 earthquake was recorded in the cable anchorage of a bridge (ca). Magnitudes as published in ISC (2001), or, when marked by an asterisk through the methodology described in the text. The references for PGA data are: (a) Ambraseys *et al.* (2002); (b) Oliveira, pers. comm. (2005); (c) IGN web page on accelerometer data.

version have been recognized for a long time. The qualitative nature of intensity scales, which bring together long-period and short-period effects, is one of the reasons advanced to explain the high scatter of the correlation between intensities and PGA (Panza *et al.*, 1997).

Atkinson and Sonley (2000) developed empirical relationships between MMI, magnitude and distance, and ground-motion parameters, for Californian earthquakes with magnitudes in the range **M** 4.9–7.4. The study reported a strong dependence on distance for high frequencies (including PGA) and a strong dependence on magnitude for low frequencies, and proposed to use such relationships to estimate the ground motions for important historical CENA earthquakes. Similarly, we converted intensities for important historical earthquakes in Western Iberia (Paula, 1996) to PGA, using the equations of Atkinson and Sonley (2000). However, very distant offshore earthquakes such as 1 November 1755 or 28 February 1969 were not considered in this analysis because their distances are largely outside the range covered by the data used to derive the empirical relations. Figures 5 and 6 show that the Atkinson and Boore (1997) curves and Toro *et al.* (1997) curves fit the converted data for the distances of interest, whereas the Ambraseys *et al.* (1996) curves tend to underpredict most of the data.

However, recent work by Kaka and Atkinson (2004) questioned the applicability of Californian intensity–ground-motion relationships to CENA, even for parameters with explicit frequency content. This finding highlights the fact that conversions between intensities and ground-motion parameters must be used with care. That notwithstanding, the fit between converted intensities and CENA attenuation models supports the use of the latter. We attributed weights of 80%

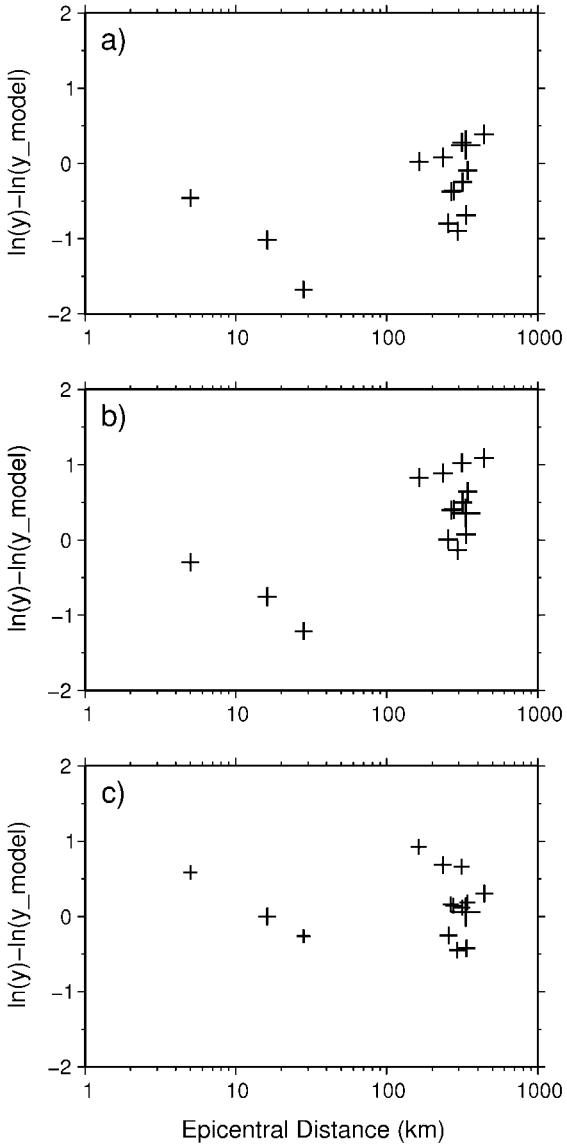

Figure 4. Residuals of the natural logarithm of PGA data on Table 6 with respect to the attenuation models used: (a) Atkinson and Boore (1997); (b) Toro *et al.* (1997); (c) Ambraseys *et al.* (1996). Amplification factors for stiff soil (1.30) and soft soil (1.33) proposed by Ambraseys *et al.* (1996) were used to account for site geology. The symbol size is proportional to the magnitude.

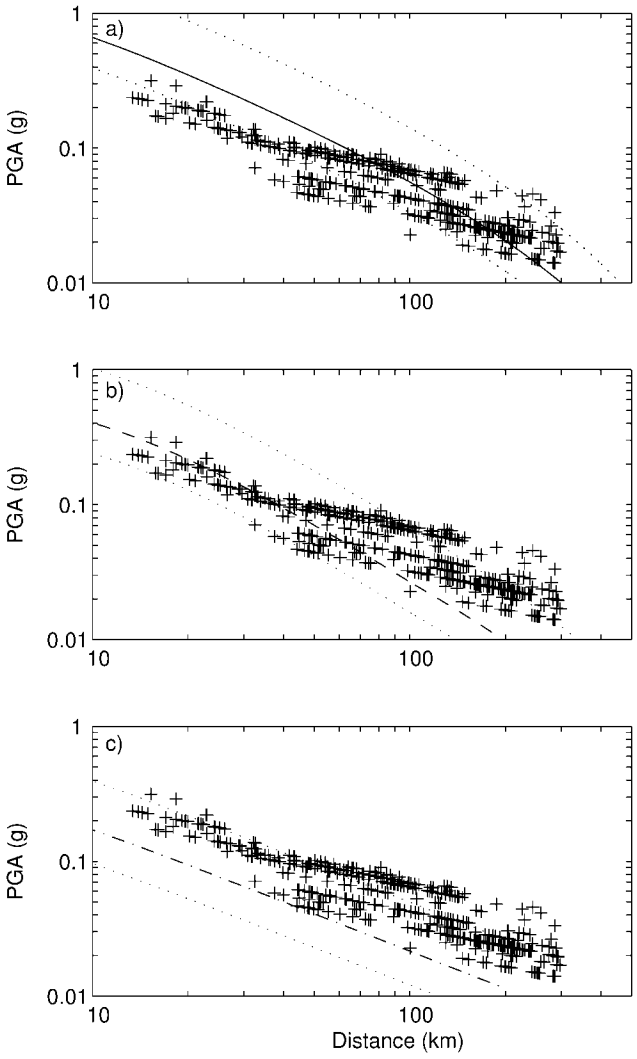

Figure 5. Data for the 23 April 1909 **M** 6.3 earthquake. The solid curves represent the model of Atkinson and Boore (1997), the dashed line is the model of Toro *et al.* (1997), and the dashed-dotted line is the model of Ambraseys *et al.* (1996). The upper and lower dotted curves represent 1.5 exp(ln $y + \sigma_y$) and exp(ln $y - \sigma_y$), where 1.5 is the soft-soil correction.

to CENA models (40% to each) and we used the model of Ambraseys *et al.* (1996) with a 20% weight because crustal age and tectonic inheritance of Western Iberia have more in common with CENA that with the Alpine Belt of Southern Europe and the Middle East.

Hazard Calculation and Uncertainty

We followed the standard approach of probabilistic seismic-hazard analysis introduced by Cornell (1968). To estimate the probability of exceedence of some specified level of ground motion, during a specific period, the distribution of earthquakes in space and size is represented through probability-density functions. The time distribution of events within each source is assumed to follow a poissonian process and the variability in the ground motion accounted for by a Gaussian distribution on the natural logarithm of the ground-motion parameter, with a standard deviation σ.

Hazard Calculations

The hazard calculations were performed with SEISRISK III (Bender and Perkins, 1987) in a 0.05° × 0.05° grid covering the region within 5.5–10° W and 36.5–42.5° N. The input recurrence rates were calculated for 0.5 magnitude in-

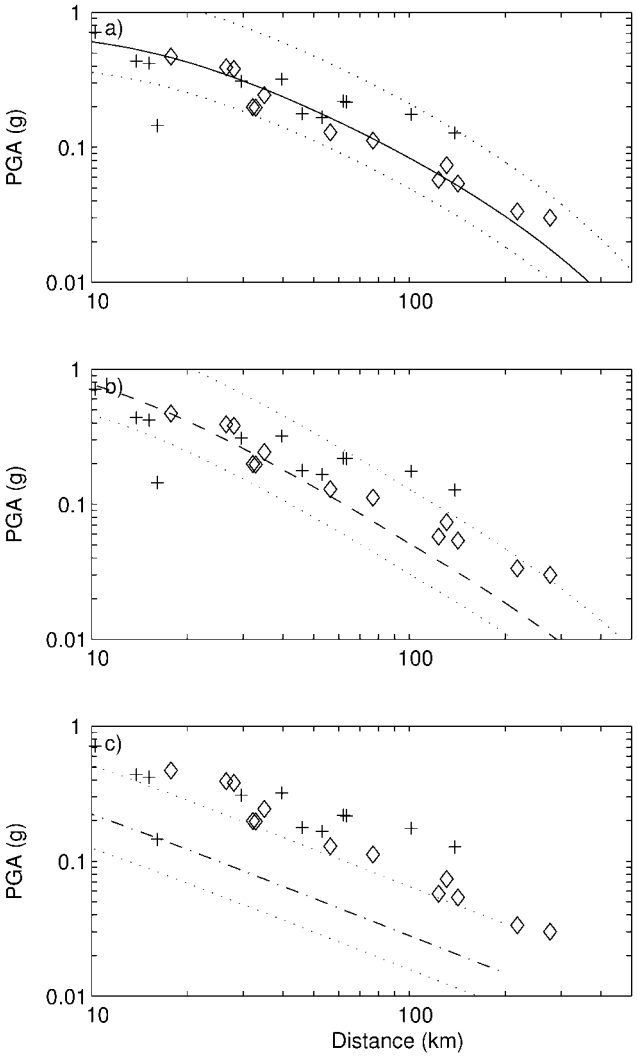

Figure 6. Data for the 26 January 1531 **M** 6.9 (crosses) and for 11 November 1858 **M** 7.1 (diamonds) earthquakes. The solid curves represent the model of Atkinson and Boore (1997), the dashed line the model of Toro *et al.* (1997), and the dashed-dotted line the model of Ambraseys *et al.* (1996). The upper and lower dotted curves represent 1.5 exp(ln $y + \sigma_y$) and exp(ln $y - \sigma_y$), where 1.5 is the soft-soil correction.

tervals above **M** 4.75 according to the exponential model characterized by the parameters in Tables 3 and 4. The attenuation table was built for 0.5 magnitude intervals in the range **M** 5.0–8.5, and for distances in the range 1.3–300 km. Rates and attenuation for any value of **M** were obtained by interpolation of these tables. A sensitivity analysis showed that smaller-magnitude steps did not change the results. The choice of such large maximum distance and maximum magnitude is related to the possibility of occurrence of very large magnitude earthquakes in seismicity zone S01 (of both zonations). This implies the extrapolation on magnitude domain in all the attenuation models considered and extrapolation beyond distance range in the attenuation model of Ambraseys *et al.* (1996). The comparison of the ground-motion model for interface subduction zone earthquakes of Youngs *et al.* (1997) with the extrapolated models shows that, for the distances of interest in S01 (100–300 km), the latter produce reasonable values of ground motion. Concerning the distances, tests showed little sensitivity to the maximum distance considered.

Aleatory and Epistemic Uncertainties

In the computation of the hazard, the variability of the ground-motion model is taken into account by integrating over the aleatory uncertainty, leading to a mean value of hazard that is higher than the value obtained using the mean ground-motion model only (Bender and Perkins, 1993). Besides the aleatory uncertainty that results from the intrinsic variability of ground motion at a particular site, the incomplete knowledge about the appropriateness of the models used and the values of their parameters contributes to the overall uncertainty affecting a hazard estimate.

When a logic tree approach is used, this epistemic uncertainty (i.e., uncertainty that can be reduced by further data acquisition and research) is represented by the multiplicity of individual results that correspond to discrete hypotheses for the models and their parameters (e.g., Reiter, 1991; Senior Seismic Hazard Analysis Committee [SSHAC], 1997). The weights assigned to the various branches of each node of the logic tree combine in such a way that the sum of the final weights is unity, and it is a standard approach to use these as the empirical probability that each estimate is the correct one. In this way, a mean (over the epistemic uncertainty) can be estimated, as well as the median and any other percentile.

This aspect of hazard evaluation has been the object of intense debate in recent years. Abrahamson and Bommer (2005) point out that the weights assigned to each hazard value in the logic tree cannot be treated strictly as probabilities, because the models sampled by the combinations of branches do not span exhaustively the model space, nor are they mutually exclusive. As a result, Abrahamson and Bommer (2005) argue against the common practice of estimating mean hazard values by weighted averages of the logic tree individual branches. This procedure is also charged with being oversensitive to low-probability high-hazard end members. McGuire *et al.* (2005), on the contrary, taking an approach based on decision theory, favor the use of mean hazard values whenever a single-hazard curve or ground-motion level has to be provided, as is the case for design.

Logic Tree

Figure 7 displays the logic tree used for the hazard calculations and the weights associated with the different branches. Zonation SA was given a larger weight because its spatial resolution seems more adequate to the current knowledge of the region. Concerning the seismicity rates, methods RA and RB were considered equivalent and the

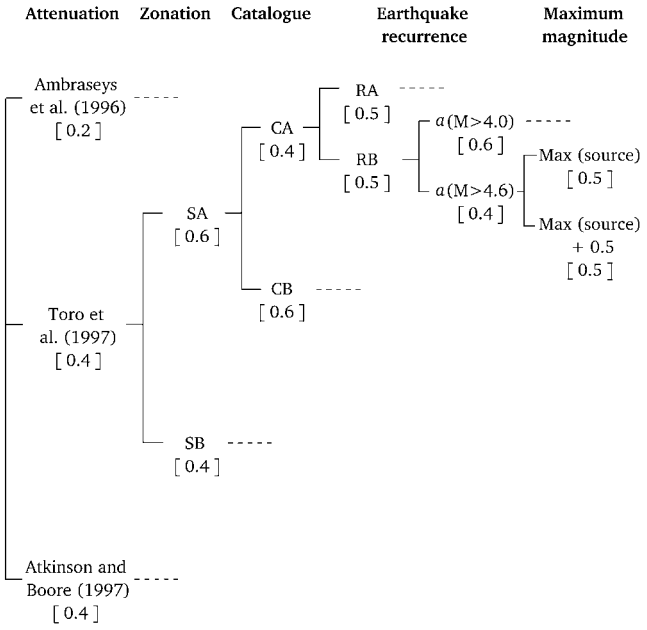

Figure 7. Logic tree used for hazard calculation. The weight of each branch is shown in straight parentheses.

combinations that included lower-quality data (version CA) were given a smaller weight relative to the stricter quality criteria (version CB). The branches related to the estimate of *a*-values in recurrence relationships using data above **M** 4.0 were considered more reliable because they included a larger amount of data. We used with the same weights the maximum magnitude equal to the historical maximum and the historical maximum increased by 0.5 magnitude units.

Concerning ground motion, the attenuation model of Ambraseys *et al.* (1996) was used with half the weight of the models of Atkinson and Boore (1997) and Toro *et al.* (1997). The attenuation models used in the logic tree are associated with different standard deviations of the natural logarithm of ground motion, as follows: 0.53 in Ambraseys *et al.* (1996); 0.53 to 0.62 (depending on frequency) in Atkinson and Boore (1997); 0.54 to 0.8 (depending on magnitude and distance) in Toro *et al.* (1997). In the latter case the higher values of σ correspond to lower magnitudes. As Bender and Perkins (1993) point out, the σ-value used in the hazard calculation for a specific site should portray the inherent variability of ground motion at that site. Because each attenuation model is derived from a specific dataset, which in the present study pertains always to a different region, the associated σ-value is not necessarily the best choice for the hazard computation. Following the procedure adopted in a wide range of hazard studies (Bender and Perkins, 1993) we used a fixed value $\sigma = 0.6$ to quantify the variability of the natural logarithm of ground motion. Although this value may be slightly conservative (Bender and Perkins, 1993), we believe it reflects adequately the large variations in seismic attenuation reported by Lopez Casado *et al.* (2000) for Portugal. A sensitivity analysis showed that varying σ within the range 0.5–0.7 produces variations of about 10% in the PGA value for 10% exceedence probability in 50 years.

Combining the parameters according to the logic tree we produced, for each point of the map, 96 hazard curves for 10% exceedence probability in 50 years.

Results and Sensitivity Analysis

In this study we followed the standard procedure of adopting the mean hazard as the final result. According to Abrahamson and Bommer (2005), their objections apply mainly to return periods longer than 2500 years, whereas this study corresponds to a return period of 475 years. For each point of the map we produced a mean hazard curve by averaging the hazard curves for the different scenarios using the associated weights. These mean hazard curves were then sampled at the reference hazard level of 10% exceedence probability in 50 years. The resulting PGA values were plotted on the mean hazard map.

Figure 8 displays the sensitivity to the choice of methods for seismic-recurrence analysis and ground-motion models and Figure 9 shows the influence of the zonation. The seismicity analysis method RB yields slightly higher ground-motion values but comparable to those obtained with method RA. The influence of the attenuation model is clearly stronger, and different attenuation models yield ground motions scattered around different mean values. This observation is in agreement with what has been observed in other hazard-sensitivity studies (e.g., Bender and Perkins, 1993; Newman *et al.*, 2001). The zonation controls the hazard pattern. Results using zonation SA show a detailed hazard pattern reaching maximum PGA values in the Lower Tagus Valley (LTV) and Algarve regions, where the contribution of local seismicity is more important. In the broader zonation SB, the hazard related to LTV is distributed over a large area, lowering considerably the PGA value. The eastern Algarve region shows an increase in the PGA value with zonation SB because it is included in the ACR tectonic zone. At this return period (475 years) the choice of maximum magnitude influences only the seismicity zones with low values of maximum observed magnitude.

Figure 10 presents the mean hazard map for the total logic tree. In addition, we used the suite of PGA values for each point and for the reference hazard level to produce 15th and 85th percentile maps. These should not be regarded as possible replacements for the mean map when a different hazard level is required (for that, a mean map for a different probability of exceedence should be used). The 15th and 85th percentile maps are proposed as brackets for plausible future evolutions of the mean map as more knowledge is gathered. The PGA exceedence values for the total logic tree vary across Portugal from 0.05*g* to 0.20*g*, whereas the 15th percentile ranges vary from 0.03*g* to 0.10*g* and the 85th percentile from 0.07*g* to 0.30*g*. The LTV and the Algarve regions display the highest hazard of Portugal.

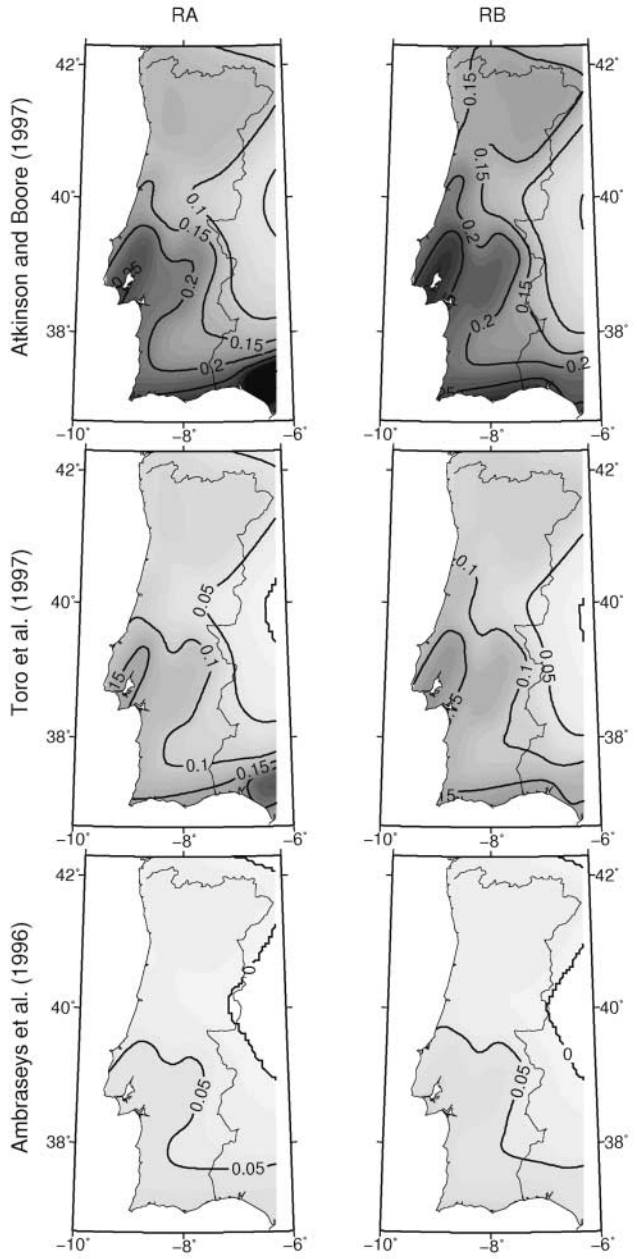

Figure 8. Partial logic tree mean hazard maps (rock) for 10% exceedence probability in 50 years. Sensitivity to the seismicity analysis method (columns) and attenuation model (rows).

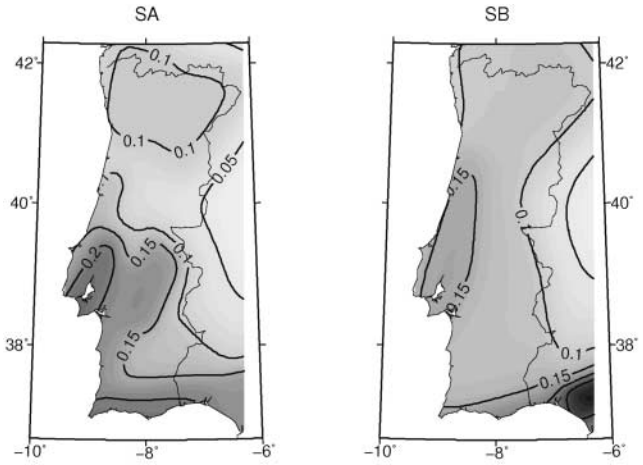

Figure 9. Partial logic tree mean hazard maps (rock) for 10% exceedence probability in 50 years. Sensitivity to the zonation.

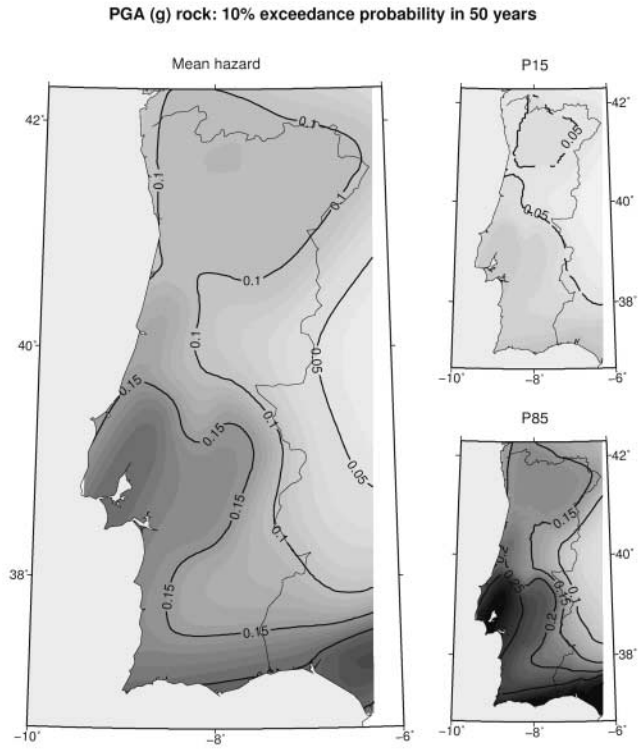

Figure 10. Mean hazard map (rock) for 10% exceedence probability in 50 years (total logic tree) and mean PGA values for the 15th and 85th percentiles (interval between different shades of gray 0.01g).

Discussion

The comparison between hazard studies is a nontrivial task because of the large number of parameters that influence the results. Figure 11 displays the seismic zonation currently in force in Portugal (Laboratorio Nacional de Engenharia Civil [LNEC], 1983), clearly dominated by the offshore scenario and hazard results from previous studies. Sousa (1996), for a 500-year return period, used local empirical attenuation models based on macroseismic intensity, obtaining the maximum hazard at the extreme southwest region of Portugal. The hazard maps of Pelaez and Lopez Casado (2002), also based on intensity attenuation models, show a similar pattern.

Oliveira *et al.* (1999) performed hazard calculations using Sousa's (1996) source characterization and Ambraseys *et al.*'s (1996) attenuation model, and the resulting hazard pattern is qualitatively similar to that obtained in the present study. Excluding the distant offshore sources, Oliveira *et al.*

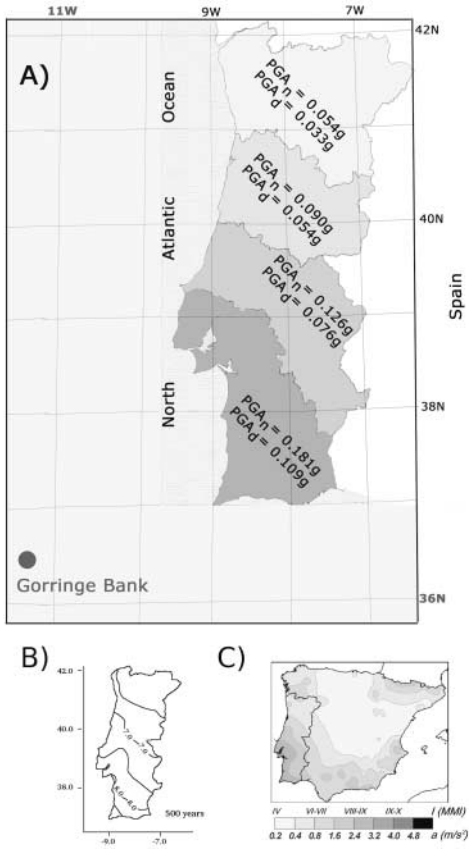

Figure 11. Previous estimates of seismic hazard for Portugal. (a) Hazard zonation currently in force, adapted from LNEC (1983); PGA values for a return period of 975 years. (b) intensities with a 500-year return period, after Sousa (1996). (c) PGA with a return period of 475 years, after Pelaez and Lopez Casado (2002).

(1999) compute PGA ranging from 0.07*g* to 0.20*g* for a 475-year return period, which is similar to our results, if slightly higher. The difference is probably because Oliveira *et al.* (1996) used nonunified magnitudes. As Ambraseys *et al.* (1996) stress, using magnitudes other than M_S in M_S-based ground-motion models will lead to higher-than-expected values of PGA.

Jimenez *et al.* (1999, 2001) present regional hazard estimates including Iberia (GSHAP and SESAME projects) but, as the authors state, in this area it was not possible to adhere fully to the GSHAP implementation guidelines of Basham and Giardini (1993). For this reason it is not clear which methodology was adopted for seismic-zone characterization. Jimenez *et al.* (2001) used the Ambraseys *et al.* (1996) attenuation model for stiff soil. The PGA values (475-year return period) obtained across Mainland Portugal are in the range 0.06–0.20*g* for stiff soil (amplification factor of 1.3 with respect to rock), meaning that Jimenez *et al.* (2001) present slightly lower hazard than that proposed by Oliveira *et al.* (1999), and even more so when compared with the present study.

Summarizing, for 10% exceedence probability in 50 years, studies based on intensity data present higher hazard values in the extreme southwest, whereas studies based on PGA data (either real or synthetic) present higher hazard on the Lower Tagus Valley and Algarve. Because the ground-motion model of Ambraseys *et al.* (1996) was derived for the most active region of Europe and the Middle East, it may not be suitable to characterize the attenuation in the old crust of Western Iberia. Also, this model seems to underestimate significantly the macroseismic data for most relevant historical earthquakes, suggesting that it is not suitable either for intraplate or interplate seismicity of Western Iberia. Empirical intensity-based attenuation models seem to lead to an overestimate of the relative importance of the distant offshore scenario, whereas PGA relationships emphasize the contribution of onshore faults to the hazard. This may be because PGA is a high-frequency parameter that does not reflect the duration of ground shaking, which becomes important at large distances. Alternatively, intensity relationships may be biased by the inclusion of very large intensities at large distances in 1755, if the proposal by Vilanova *et al.* (2003) of a triggered onshore event is correct.

Conclusions and Remarks

By critically reviewing the seismicity catalog for southwest Iberia, using judiciously the available data to select appropriate attenuation relations, we produced a probabilistic assessment of the seismic hazard for Portugal and quantified the associated uncertainty using a logic tree approach. For the mean hazard map we obtained a range of values from 0.05*g* to 0.20*g* for the PGA in rock with 10% exceedence probability in 50 years (return period of 475 years). Considering the 85th percentile the values range from 0.07*g* to 0.30*g*. The highest PGA values correspond to the Lower Tagus Valley region, near Lisbon, and the Algarve. This contrasts with previous studies based on intensity, which assign the highest hazard to the southwest Algarve.

The completeness analysis requires a substantial judgment by the analyst, and therefore the use of methods RA and RB accounts for a significant part of the scatter in the hazard results. However, the uncertainty of seismic-hazard assessment in Portugal is clearly dominated by the uncertainty of ground-motion attenuation models. Further improvements will require the study of the crustal properties and the characteristics of wave propagation in the region. The large uncertainties affecting the magnitude and epicentral location of the 1 November 1755 Lisbon earthquake are also a hindrance to accurate hazard assessment (Fonseca, 2005). However, in view of the slow (4 mm/yr) rate of convergence between Africa and Eurasia, such a large event has to be associated with a long-return period, thus having a limited impact in the present study. Hazard assessment for lower hazard levels, on the other hand, must address this issue with great care.

Another important issue concerns the inclusion of fault sources in the probabilistic hazard analysis. Previous studies that included the Lower Tagus Valley fault zone to account for magnitudes **M** 6.5–7.0 (using the exponential recurrence model seismicity rates) showed a local increase of about 50% in the PGA (Vilanova and Fonseca, 2004). More sophisticated models like the characteristic earthquake need input data from paleoseismology (Holocene slip rates, event magnitude, and time of last rupture). It is therefore necessary to invest in paleoseismological characterization of the active faults, in particular in regions that display moderate- to high-magnitude seismicity like the Lower Tagus Valley and the Algarve.

Acknowledgments

One of the authors (S.P.V.) acknowledges a post-doc research grant by Fundação para a Ciência e a Tecnologia (contract SFRH/BPD/19287/2004). Part of the research was conducted within the scope of projects TAGUS and TAGUS2 of program POCTI (FCT), partly funded by the European Union (ERDF). Many discussions with Carlos Sousa Oliveira and Vittorio Bosi contributed to the results presented. Part of the research was conducted while one of the authors (S.P.V.) was visiting Servizio Sismico Nazionale, Rome. Most of the figures were drawn using the Generic Mapping Tools software of Wessel and Smith (1991). Comments by two anonymous reviewers and by Associate Editor Ivan Wong helped us to improve the manuscript.

References

Abrahamson, N., and J. Bommer (2005). Probability and uncertainty in seismic hazard analysis, *Earthquake Spectra* **21,** 603–607.

Albarello, D., R. Camassi, and A. Rebez (2001). Detection of space and time heterogeneity in the completeness of a seismic catalog by a statistical approach: an application to the Italian area, *Bull. Seism. Soc. Am.* **91,** 1694–1703.

Ambraseys, N., K. Simpson, and J. Bommer (1996). Prediction of horizontal response spectra in Europe, *Earthquake Eng. Struct. Dyn.* **25,** 371–400.

Ambraseys, N., P. Smit, R. Sigbjornsson, P. Suhadolc, and B. Margaris (2002). Internet-Site for European Strong-Motion Data, European Commission, Research-Directorate General, Environment and Climate Programme, Bruxelles.

Argus, D., R. Gordon, R. DeMets, and C. Stein (1989). Closure of Africa-Eurasia-North America Plate motion circuits and tectonics of the Gloria fault, *J. Geophys. Res.* **94,** 5585–5602.

Arthaud, F., and P. Matte (1975). Les decrochements tardi-Hercyneens du sud-ouest de l'Europe: geometrie et essai de reconstruction des conditions de deformation, *Tectonophysics* **25,** 139–171.

Atkinson, G., and D. Boore (1997). Some comparisons between recent ground motion relations, *Seism. Res. Lett.* **68,** 24–40.

Atkinson, G., and E. Sonley (2000). Empirical relationships between Modified Mercalli intensity and response spectra, *Bull. Seism. Soc. Am.* **90,** 537–544.

Basham, P., and D. Giardini (1993). Technical guidelines for global seismic hazard assessment, *Ann. Geofis.* **36,** 15–24.

Bender, B., and D. Perkins (1987). SEISRISK III: a computer program for seismic hazard estimation, *U.S. Geol. Surv. Bull. 1772*.

Bender, B., and D. Perkins (1993). Treatment of parameter uncertainty and variability for a single seismic hazard map, *Earthquake Spectra* **9,** 165–195.

Buforn, E., C. Sanz de Galdeano, and A. Udias (1995). Seismotectonics of the Ibero-Maghrebian region, *Tectonophysics* **248,** 247–261.

Cabral, J. (1989). An example of intraplate neotectonic activity, Vilariça basin, northeast Portugal, *Tectonics* **8,** 285–303.

Cabral, J. (1995). A Neotectónica em Portugal Continental, Instituto Geológico e Mineiro, Memoir 31, Lisbon.

Cabral, J., and F. Marques (2001). Paleoseismological studies near Lisbon: Holocene thrusting or landslide activity?, *EOS Trans. AGU* **82,** 351–353.

Centre Sismologique Euro-Mediterraneen/European-Mediterranean Seismological Centre (CSEM/EMSC) (1999). European-Mediterranean Seismological Centre, Newsletter 15, Bruyeres-le-Chatel, France.

Cornell, C. (1968). Engineering seismic risk analysis, *Bull. Seism. Soc. Am.* **58,** 1568–1606.

Dineva, S., J. Batllo, D. Mihaylov, and T. Van Eck (2002). Source parameters of four strong earthquakes in Bulgaria and Portugal at the beginning of the 20th century, *J. Seism.* **6,** 99–123.

Feraud, G., D. York, C. Mevel, G. Cornen, C. Hall, and J. Auzende (1986). Additional 40Ar 39Ar dating of the basement and alkaline volcanism of Gorringe Bank (Atlantic Ocean), *Earth Planet. Sci. Lett.* **79,** 255–269.

Fonseca, J. (2005). The source of the Lisbon earthquake (letter), *Science* **308,** 5–6.

Fonseca, J., V. Bosi, S. Vilanova, and M. Meghraoui (2000). Paleoseismological investigations unveil Holocene thrusting onshore Portugal, *EOS Trans. AGU* **81,** 412–413.

Frankel, A. (1995). Mapping seismic hazard in the central and eastern United States, *Seism. Res. Lett.* **66,** 8–21.

Fukao, Y. (1973). Thrust faulting at a Lithospheric plate boundary: the Portugal earthquake of 1969, *Earth Planet. Sci. Lett.* **18,** 205–216.

Grimison, N., and W. P. Chen (1986). The Azores-Gibraltar plate boundary: focal mechanisms, depths of earthquakes, and their tectonic implications, *J. Geophys. Res.* **91,** 2029–2047.

Hanks, T., and H. Kanamori (1979). A moment magnitude scale, *J. Geophys. Res.* **84,** 2348–2350.

Instituto Geografico Nacional (IGN) (1992). *The Seismicity Catalog*, CD-ROM Collection, National Earthquake Information Center, Golden, Colorado.

International Seismological Center (ISC) (2001). International Seismological Centre On-line Bulletin, International Seismological Centre, Thatcham, United Kingdom

Jimenez, M., and M. Garcia Fernandez, and GSHAP Ibero-Maghreb Working Group (1999). Seismic hazard assessment in the Ibero-Maghreb region, *Ann. Geofis.* **42,** 1057–1066.

Jimenez, M., D. Giardini, and G. Grunthal, and SESAME Working Group (2001). Unified sesmic hazard modelling throughout the Mediterranean region, *Boll. Geofis.* **42,** 3–18.

Johnston, A. (1989). The seismicity of "Stable Continental Interiors," in *Earthquakes at North-Atlantic Passive Margins: Neotectonics and Postglacial Rebound*, S. Gregersen and P. Basham (Editors), Kluwer Academic Publishers, Norwell, Massachusetts, 299–327.

Johnston, A. (1996a). Seismic moment assessment of earthquakes in stable continental regions—I. Instrumental seismicity, *Geophys. J. Int.* **124,** 381–414.

Johnston, A. (1996b). Seismic moment assessment of earthquakes in stable continental regions—II. Historical seismicity, *Geophys. J. Int.* **125,** 639–678.

Johnston, A. (1996c). Seismic moment assessment of earthquakes in stable continental regions—III. New Madrid 1811–1812, Charleston 1886 and Lisbon 1755, *Geophys. J. Int.* **126,** 314–344.

Johnston, A., and L. Kanter (1990). Earthquakes in stable continental interiors, *Scientific American* **262,** 68–75.

Justo, J. L., and P. Gentil (1990). El terramoto peninsular del 24 de Agosto de 1356, *Ingen. Civil* **74,** 34–42.

Justo, J. L., and C. Salwa (1998). The 1531 Lisbon earthquake, *Bull. Seism. Soc. Am.* **88,** 319–328.

Kaka, S., and G. Atkinson (2004). Relationships between instrumental ground-motion parameters and modified mercalli intensity in Eastern North America, *Bull. Seism. Soc. Am.* **94,** 1728–1736.

Laboratorio Nacional de Engenharia Civil (LNEC) (1983). *Regulamento de Segurança e Acções para Estruturas de Edifícios e Pontes*, Ed. Imprensa Nacional-Casa da Moeda, Lisbon.

Lopez Casado, C., S. Palacios, J. Delgado, and J. Pelaez (2000). Attenuation of intensity with epicentral distance in the Iberian Peninsula, *Bull. Seism. Soc. Am.* **90,** 34–47.

Machado, F. (1966). Contribuição para o estudo do terramoto de 1 de Novembro de 1755, *Rev. Fac. Cien. Lisboa C* **14,** 19–31.

Martinez Solares, J., and A. Lopez Arroyo (2004). The great historical 1755 earthquake, effects and damage in Spain, *J. Seism.* **8,** 275–294.

Martins, I., and L. Mendes-Victor (1990). Contribuição para o Estudo da Sismicidade de Portugal Continental, Instituto Geofísico Infante D. Luís, Memoir 18, Lisbon.

McCalpin, J. (1996). Application of paleoseismic data to seismic hazard assessment and neotectonic research, in *Paleoseismology*, J. McCalpin (Editor), Academic Press, New York, 439-493.

McGuire, R., C. Cornell, and G. Toro (2005). The case for using mean seismic hazard, *Earthquake Spectra* **21,** 879–886.

McKenzie, D. (1970). Plate tectonics of the Mediterranean region, *Nature* **226,** 239–243.

Mezcua, J., and J. Martinez Solares (1983). Sismicidad del area Ibero-Mogrebi, Instituto Geografico Nacional, Memoir 203, Madrid.

Moreira, V. (1979). Contribuiçao para o conhecimento da sismicidade historica de Portugal Continental, *Revista do Instituto Nacional de Metereologia e Geofisica* (special issue), Instituto Nacional de Metereologia e Geofisica, Lisbon, Portugal.

Moreira, V. (1989). Seismicity of the Portuguese continental margin, in *Earthquakes at North-Atlantic Passive Margins: Neotectonics and Postglacial Rebound*, S. Gregersen and P. Basham (Editors), Kluwer Academic Publishers, 533–545.

Newman, A., J. Schneider, S. Stein, and A. Mendez (2001). Uncertainties in seismic hazard maps for the New Madrid seismic zone and implications for seismic hazard communication, *Seism. Res. Lett.* **72,** 647–663.

Oliveira, C. S. (1986). A simicidade histórica e a revisão do catálogo sísmico, Laboratório Nacional de Engenharia Civil, Proc. 36/11/7368, Lisbon.

Oliveira, C. S., M. Sousa, and A. Costa (1999). Contribuição para a revisão da acção sísmica em Portugal Continental no contexto do eurocódigo 8, in *4° Encontro Nacional de Sismologia e Engenharia Sísmica e 2eme Rencontre en Génie Parasismique des Pays Méditerranés — Sismica 99*, C. A. Martins (Editor), Univ. Algarve, Faro, 153–164.

Panza, G., F. Vaccari, and R. Cazzaro (1997). Correlation between macroseismic intensities and seismic ground motion parameters, *Ann. Geofis.* **15,** 1371–1382.

Paula, A. (1996). Base de Dados de Informação Macrossísmica, Report to the CEC Environment Program EV5V-CT94-0443, Instituto Superior Técnico, Lisbon.

Pelaez, J., and C. Lopez Casado (2002). Seismic hazard estimate at the Iberian Peninsula, *Pure Appl. Geophys.* **159,** 2699–2713.

Pinheiro, L., R. Whitmarsh, and P. Miles (1992). The ocean-continent boundary off the werstern continental margin of Iberia — II. Crustal structure in the Tagus Abyssal Plain, *Geophys. J. Int.* **109,** 106–124.

Pinheiro, L., R. Wilson, R. Pena dos Reis, R. Whitmarsh, and A. Ribeiro (1996). The Western Iberian Margin: a geophysical and geological overview, in *Proceedings of the Ocean Drilling Program, Leg 149, Scientific Results Volume*, R. Whitmarsh, D. Daywer, A. Klaus, and D. Masson (Editors), IODP, Washington, 533–545.

Reiter, L. (1991). *Earthquake Hazard Analysis: Issues and Insights*, Columbia University Press, New York.

Ribeiro, A., M. Antunes, M. Ferreira, R. Rocha, A. Soares, G. Zbyszewski, F. Moitinho de Almeida, D. Carvalho, and J. Monteiro (1979). *Introdution À la Geologie Génerale Du Portugal*, Ed. Serv. Geol. Portugal, Lisbon.

Rockwell, T., C. Madden, and E. Gath (2005). Results of the fault trenching investigation to assess the potential seismic hazard of the Vilariça fault, northwestern Portugal, Earth Consultants International, Tustin, California, contract 2505.

Senior Seismic Hazard Analysis Committee (SSHAC) (1997). Recommendations for probabilistic seismic hazard analysis: guidance on uncertainty and use of experts, U.S. Nuclear Regulatory Commission, Report NUREG/CR-6372.

Sousa, M. L. (1996). Modelos Probabilistas Para Avaliação Da Casualidade Sísmica Em Portugal Continental, *M.Sc. Thesis*, Instituto Superior Técnico, Lisbon.

Sousa, M. L., A. Martins, and C. S. Oliveira (1992). Compilação de catálogos sísmicos da região Ibérica, Laboratório Nacional de Engenharia Civil, Proc. 36/11/9295, Lisbon.

Stepp, J. C. (1972). Analysis of completeness in the earthquake sample in the Puget Sound area and its effect on statistical estimates of seismic hazard, in *Proceedings of the International Conference on Microzonation for Safer Construction Research and Applications*, Vol. 2, Seattle, Washington, 1897–1910.

Toro, G., N. Abrahamson, and J. Schneider (1997). Model of strong ground motions from earthquakes in central and eastern North America: best estimates and uncertainties, *Seism. Res. Lett.* **68,** 41–57.

Triep, E., and L. Sykes (1997). Frequency of occurrence of moderate to great earthquakes in intracontinental regions: implications for changes in stress, earthquake prediction, and hazards assessments, *J. Geophys. Res.* **102,** 9923–9948.

Udias, A., A. Lopez Arroyo, and J. Mezcua (1976). Seismotectonic of the Azores—Alboran region, *Tectonophysics* **31,** 259–289.

Vilanova, S. (2004). Sismicidade e Perigosidade Sísmica no Vale Inferior do Tejo, *Ph.D. Thesis*, Instituto Superior Técnico, Lisbon.

Vilanova, S., and J. Fonseca (2004). Seismic hazard impact of the Lower Tagus valley fault zone (SW Iberia), *J. Seism.* **8,** 331–345.

Vilanova, S., C. Nunes, and J. Fonseca (2003). Lisbon 1755: a case of triggered onshore rupture?, *Bull. Seism. Soc. Am.* **93,** 2056–2068.

Weichert, D. (1980). Estimation of the earthquake recurrence parameters for unequal observation periods for different magnitudes, *Bull. Seism. Soc. Am.* **70,** 1337–1346.

Wells, D., and K. Coppersmith (1994). New empirical relationships among magnitude, rupture length, rupture width, rupture area, and surface displacement, *Bull. Seism. Soc. Am.* **84,** 974–1002.

Wessel, P., and W. Smith (1991). Free software helps map and display data, *EOS Trans. AGU* **72,** 441.

Youngs, R., S.-J. Chiou, W. Silva, and J. Humphrey (1997). Strong ground motion attenuation relationships for subduction zone earthquakes, *Seism. Res. Lett.* **68,** 58–73.

Earthquake Engineering and Seismology Division
Instituto de Engenharia de Estruturas, Territorio e Contruçao (ICIST),
Instituto Superior Técnico
1049-001 Lisbon, Portugal
(S.P.V.)

Physics Department, Instituto Superior Técnico
1049-001 Lisbon, Portugal
(J.F.B.D.F.)

Manuscript received 30 September 2005.